PHYSICAL REVIEW B VOLUME 26, NUMBER 9 1 NOVEMBER 1982

NMR study of tunneling states in solid CD_4

Saps Buchman, W. T. Vetterling, Donald Candela, and R. V. Pound
Lyman Laboratory of Physics, Harvard University, Cambridge, Massachusetts 02138
(Received 12 April 1982)

We report an NMR study of solid CD_4 in the temperature range 35–455 mK. At the lower temperatures, the area of the NMR absorption line shows a significant increase over that expected from the Curie law alone. We interpret this as evidence for spin-species conversion, associated with the thermal relaxation of the occupation of an array of tunneling levels. The width of the NMR line increases at low temperatures, and this increase is consistent with the increase in the intermolecular second moment due to spin-species conversion. Our data are compared with the predictions of models for the tunneling levels which were developed on the basis of neutron scattering experiments. We also present measurements of the nuclear spin-lattice relaxation time and of the spin-species conversion time.

I. INTRODUCTION

In the presence of a crystalline field, a symmetrical molecule such as methane will have several equivalent orientations corresponding to the lowest potential energy. States of the molecule which are localized in a particular one of these orientations are not eigenstates of the orientational Hamiltonian, because of the quantum-mechanical probability of tunneling between different orientations. The eigenstates may be approximated by linear combinations of states localized in particular orientations, and are referred to as "tunneling states."[1,2]

Solid ordinary methane (CH_4) undergoes a phase transition at 20.4 K.[3] In the low-temperature phase, which is called CH_4 II, $\frac{3}{4}$ of the molecules experience a collective molecular field which strongly hinders their rotation, while the remaining $\frac{1}{4}$ of the molecules remain essentially free rotors. This unusual structure was first predicted by James and Keenan on the basis of a classical mean-field theory which included only octupole-octupole interactions between the molecules.[4] (The octupole moment is the lowest nonvanishing electrostatic moment of a tetrahedral molecule.) Yamamoto *et al.* have shown that the same structure is predicted for CH_4 II (and CD_4 II) by the quantum mean-field theory they have developed.[5] Their theory uses a more complex and realistic intermolecular potential, and also allows proper treatment of symmetry under interchange of identical nuclei.

Excitations of the rotationally hindered molecules in CH_4 II out of their orientational ground states in the molecular field are called librons, and have a characteristic energy of about 70 K. The librational ground state exhibits tunneling splittings of about 1 K. The existence of these tunneling splittings has been verified by Glattli *et al.*[6] in an NMR experiment which showed resonant relaxation by level crossing with paramagnetic impurities, and by Press and Kolmar in a neutron scattering experiment.[7]

When the hydrogen in CH_4 is replaced with deuterium, the molecular wave functions become more highly localized about minima in the orientational potential because of the increased moment of inertia of the molecule. As a result, the probability of tunneling between equivalent orientations and thus the tunneling splittings are greatly reduced. Huller and Raich have estimated that the tunneling splittings for CD_4 should be about 50 times smaller than the corresponding splittings for CH_4.[8] Unfortunately, this prediction cannot be tested directly because CD_4 II only exists in the temperature range 22.1–27.0 K. At 22.1 K, CD_4 undergoes a second transition into a new phase called CD_4 III.[3] Maki *et al.* have predicted a structure for CD_4 III on the basis of classical mean-field theory,[9] but Prager *et al.* find this structure to be inconsistent with their neutron scattering data.[10] CD_4 III exhibits a slight tetragonal distortion,[11] and it is presumed that all of the molecules are rotationally hindered because of the reduced lattice symmetry. This means that all of the molecules will show tunneling splittings.

White and Morrison[12] attributed an excess specific heat below 0.5 K to an array of tunneling states with a maximum splitting of 42 ± 10 mK. In a neutron scattering experiment, Press *et al.*[13] saw evidence for four tunneling transitions in CD_4 at 14, 26, 33, and 40 mK. More recently, using an extended energy scan, Prager, Press, and Heidemann[10] (PPH) observed at least four further transitions ex-

tending in energy up to 92 mK. In order to account for the complex spectra, they introduced a number of alternative models involving from two to five inequivalent lattice sites.

In this paper we report an NMR study of CD_4 III in the temperature range 35–455 mK. The various tunneling states have different expectation values of the squared nuclear spin $\langle I(I+1)\rangle$. Changes with temperature of the populations of the tunneling states may thus be monitored by measuring the nuclear magnetic susceptibility. The second moment of the NMR line also depends upon $\langle I(I+1)\rangle$, providing further evidence of tunneling transitions. In Sec. II of this paper, we summarize the models of tunneling splittings in CD_4 developed by PPH and we show how NMR measurements can give information about the actual tunneling splittings in the solid. In Sec. III we describe our experimental procedures and present our results. Measurements of the NMR line area and line width are compared with the predictions of the models of Sec. II. Measurements of the spin-species conversion time and of the nuclear spin-lattice relaxation time are also presented.

II. THEORETICAL OVERVIEW

A. Tunneling states and nuclear-spin symmetry

The orientational states of a molecule with tetrahedral symmetry may be labeled by the representation [A, F, or $E=(E_1,E_2)$] of the group T to which they belong. (Sometimes the group T_d, which includes improper rotations, is used for computations.) For CH_4 or CD_4, the total wave function (including nuclear spin) must transform according to the totally symmetric A representation of T. This in turn implies that the nuclear spin state belongs to the same representation as the orientational state. Transition rates between states belonging to different representations are inhibited because they involve a simultaneous nuclear and orientational transition. Thus, both CH_4 and CD_4 have three long-lived "spin species," A, F, and E.

At $\frac{3}{4}$ of the sites in the low-temperature phase of CH_4, and presumably at all of the sites in the low-temperature phase of CD_4, there is a strong orientational potential (on the order of 100 K). In the presence of such a potential, the ground eigenstates of the orientational Hamiltonian are highly localized in the minima of the potential. In the absence of overlap of the wave functions for adjacent minima, the orientational ground state is 12-fold degenerate because of the 12 proper rotations that take a tetrahedron into itself. Under the group T, these states transform like one (one-dimensional) A representation, three (three-dimensional) F representations, and one (two-dimensional) E representation. Nagamiya[1] showed how the presence of small overlaps between the wave functions localized in the 12 equivalent minima of the orientational potential leads to tunneling splittings between the A, F, and E states. With the use of the notation of Huller,[14] a given orientational potential is characterized by four overlap matrix elements h_1,h_2,h_3,h_4 for 120° rotations about the four threefold axes of the molecule, and by three overlap matrix elements H_x,H_y,H_z for 180° rotations about the three twofold axes of the molecule.

When nuclear spin and the requirements of permutation symmetry are taken into account, it is found that only certain values of the total nuclear spin I are associated with each spin species. For CD_4, the resulting degeneracies of the tunneling states (and associated I values) of the three spin species are as follows: A, 15 ($I=0,2,4$); F, 54 ($I=1,2,3$); E, 12 ($I=0,2$). Because each spin species is associated with more than one value of I, the latter is not in general a good quantum number in CD_4.

B. Site models for CD_4 III

PPH have introduced a number of alternative models of the tunneling splittings present in CD_4 III, on the basis of incoherent neutron scattering at 4.2 K.[10] The five models they consider most plausible (which they call "models 1, 2, 2a, 3, and 4") each involve from two to five inequivalent sites in the solid. In all of these models, the 180° overlap matrix elements H_x,H_y,H_z are considered negligible compared to the 120° overlap matrix elements h_1 through h_4. Under this assumption, the energy of the E states is $-h=-(h_1+h_2+h_3+h_4)$, the energy of the A states is $2h$, and the mean energy of the F states is zero. (All of the overlap matrix elements are negative, so the A states are lowest in energy.) If h_1 h_2, h_3, and h_4 are all equal, the F states are degenerate at zero energy. The effect of inequality among h_1 through h_4 is to split the F states into two or three groups.[14] The NMR measurements we will present are not in general very sensitive to this F state splitting, so we will introduce a simplified model of the tunneling splittings in CD_4 III, with only one type of site and with no F state splitting. This model, which we will call model 0, has only a

single adjustable parameter, h. Below we will fit this parameter to our NMR measurements, and consider the implications for the multisite models 1 through 4 derived by PPH on the basis of neutron scattering. Figure 1 summarizes the tunneling splittings for each model.

C. Nuclear magnetic susceptibility

The nuclear magnetic susceptibility, and thus the area of the NMR absorption line, is proportional to $\langle I(I+1)\rangle/T$, where T is the temperature. The expectation value $\langle I(I+1)\rangle$ is 8.0 for the high-temperature equilibrium mixture of spin species, while $\langle I(I+1)\rangle$ is 14.0 for the A species alone. This means that spin-species conversion at temperatures comparable to the tunnel splittings will be manifested by an increase in the NMR area above that expected from the Curie law. The exact temperature dependence of $\langle I(I+1)\rangle$ will depend upon the details of the tunneling level structure.

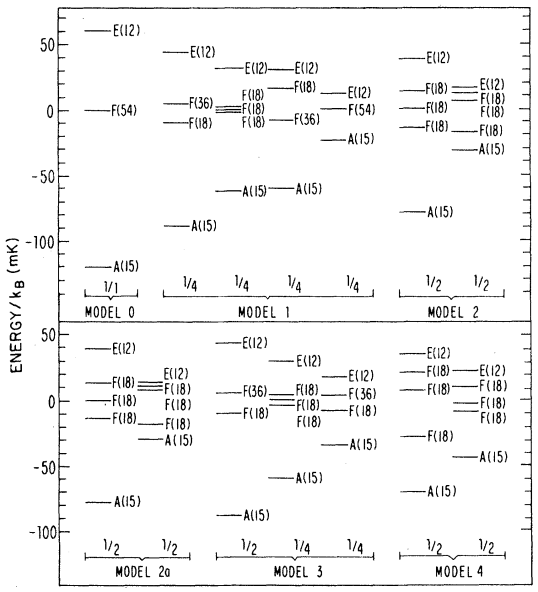

FIG. 1. Tunneling levels in CD_4 II predicted by six models of the molecular field in the solid. Models 1 through 4 were developed by Prager *et al.* (Ref. 10) on the basis of a neutron scattering experiment. Each of these models involves several inequivalent sites. Model 0 is a simplified one-site model used to analyze the NMR data reported in this paper. The number under each set of levels indicates the fraction of the molecular sites which have this level structure. The notation to the right of each level shows the representation to which it belongs and its degeneracy.

This allows our measurements to be checked for consistency with the various models.

This simple picture is complicated by the interaction of the quadrupole moment of the deuteron with the electric field gradient of the methane molecule. This interaction is on the order of 100 kHz in frequency units,[15] and can broaden the NMR line enough to make it unobservable. Both the A states and the E states have probability amplitudes distributed equally over all 12 possible orientations of the molecule, so the quadrupole interaction vanishes for these states. There are three substates in each F representation, and the quadrupole interaction vanishes for an average over these substates but not for the individual substates.[16] This means that the F states will contribute a narrow NMR line only if transitions between the F substates are fast compared with the frequency associated with the quadrupole interaction. Such fast transitions are to be expected, because of the size of the fluctuation terms ignored in the mean-field-theory treatment of the phase transition in solid methane. If the F states do contribute an unobserved wide component to the NMR line, then the apparent temperature dependence of $\langle I(I+1)\rangle$ arising from the A and E states is very different from that expected if the F states are observed [for example, the ratio of the zero-temperature value of $\langle I(I+1)\rangle$ to the high-temperature value is 4.2 rather than 1.75]. The fast- and slow-transition cases may thus be distinguished by NMR line-area measurements.

D. The second moment

If, following the discussion above, we assume that the quadrupole interaction of the deuteron makes no contribution to the observed NMR linewidth, then the internuclear dipole-dipole interaction will effectively determine the NMR line shape. This interaction may be divided into intramolecular and intermolecular parts. We are not aware of any calculation of the intramolecular second moment, although it has long been known that the intramolecular dipole-dipole interaction vanishes for the A spin species.[16] Piott and McCormick[17] attributed an anomalous temperature dependence of the second moment in CH_4 II to the intramolecular interactions, but Nijman and Trappeniers[18] showed that the temperature dependence could be explained by the differing spin-species conversion rates for the two types of molecular sites in phase II. The smallness of the intramolecular contribution to the second moment is apparently due to

the nature of the tunneling-state wave functions, which average the dipole-dipole interaction over all 12 equivalent orientations of the molecule in the molecular field.

Nijman and Trappeniers[18] have derived the following expression for the second moment due to intermolecular dipole-dipole interactions:

$$M_{ab}=\tfrac{3}{5}\gamma^4\hbar^2R_{ab}^{-6}\frac{2\langle I(I+1)\rangle_a\langle I(I+1)\rangle_b}{\langle I(I+1)\rangle_a+\langle I(I+1)\rangle_b}\ . \tag{1}$$

Here M_{ab} is the contribution of molecule b to the second moment of the NMR line of molecule a, γ is the deuteron gyromagnetic ratio, R_{ab} is the distance between the centers of molecules a and b, and $\langle I(I+1)\rangle_{a(b)}$ is the expectation value of the squared nuclear angular momentum for molecule a (b). This formula is for a powder specimen, in which all possible orientations of the intermolecular vector are equally represented. If the spin-species conversion rate were fast compared to the frequency associated with the dipole interactions (about 1 kHz), then the expectation values $\langle I(I+1)\rangle_{a(b)}$ in this formula would be thermal averages over all three spin species. We find experimentally that the conversion rate is much slower than this (typically $10^{-3}\,\mathrm{sec}^{-1}$). In this case each molecule's NMR line has a different second moment, depending upon the spin species of the molecule and that of its neighbors. When we sum Eq. (1) over all neighbors for an fcc lattice, and average it over all possible spin species combinations, we obtain the following expression for the intermolecular second moment:

$$\begin{aligned}M_2=&(14.50)(\tfrac{3}{5})\gamma^4\hbar^2R^{-6}\\&\times(p_A^2I_{AA}+p_F^2I_{FF}+p_E^2I_{EE}+2p_Ap_FI_{AF}\\&+2p_Fp_EI_{FE}+2p_Ap_EI_{AE})\ .\end{aligned} \tag{2}$$

Here p_i is the probability of a molecule belonging to the ith spin species, R is the nearest-neighbor distance, and I_{ij} is given by

$$I_{ij}=\frac{2\langle I(I+1)\rangle_i\langle I(I+1)\rangle_j}{\langle I(I+1)\rangle_i+\langle I(I+1)\rangle_j}\ , \tag{3}$$

where $\langle I(I+1)\rangle_A=14$, $\langle I(I+1)\rangle_F=7$, and $\langle I(I+1)\rangle_E=5$. If the molecules in F states are unobserved because of quadrupolar broadening, the second moment of the observed A and E molecules will still reflect the presence of the F molecules. In this case we must replace Eq. (2) with the following formula for the average second moment of the observed molecules:

$$\begin{aligned}M_2'=&(14.50)(\tfrac{3}{5})\gamma^4\hbar^2R^{-6}(p_A+p_E)^{-1}\\&\times(p_A^2I_{AA}+p_E^2I_{EE}+2p_Ap_EI_{AE}+p_Ap_FI_{AF}\\&+p_Fp_EI_{FE})\ .\end{aligned} \tag{4}$$

The actual second moment of the CD_4 deuteron NMR line is expected to be very large and unrelated to the dipolar second moment computed above. This is because the F states are presumed to give a narrow line despite their large quadrupole interactions, due to fast transitions among the F substates. As is well known, the second moment is invariant under motional narrowing.[19] Thus, the quadrupole interactions must contribute a large second moment in the form of unobservable, Lorentzian wings to the NMR line. Rather than attempting to compute the second moment of the observed lines, it is preferable to plot an unambiguous quantity such as the full width at half maximum (FWHM) versus the square root of the computed second moment. If the shape of the line is relatively temperature independent, the two quantities should be proportional, and the constant of proportionality should be on the order of 1.

E. Spin-lattice relaxation time

Nijman *et al.*[20] and Sprik and Trappeniers[21] have calculated the nuclear spin-lattice relaxation time T_1 for CH_4 II. However, the deuteron quadrupole moment is expected to give rise to powerful relaxation mechanisms that overshadow the dipolar relaxation mechanisms considered by these authors. The quadrupole interaction vanishes for the A and E spin species, but transitions between the substates associated with the F species can give rise to nuclear relaxation. de Wit and Bloom[15] observed a pronounced minimum in the CD_4 deuteron T_1 at a temperature of about 15 K, for a Larmor frequency of 4.4 MHz. This suggests that the molecular reorientations may be characterized by a temperature-dependent correlation time which equals the Larmor period at the temperature of the T_1 minimum. Under the assumption of an exponential correlation function, T_1 should be approximately proportional to the square of the Larmor frequency at temperatures well below the temperature of the minimum. However, if the correlation time becomes very long, the NMR line of the F molecules will exhibit a quadrupolar broadening. The width of a motionally narrowed NMR line is approximately M_2t_c, where M_2 is the (motionally invariant) second moment and t_c is the correlation time of the motion.[19] The classical (fixed molecule)

quadrupolar second moment may be estimated to be $(M_2)^{1/2} \simeq 50$ kHz. The maximum relaxation rate measured by de Wit and Bloom is about 30 times smaller than their classical calculation predicts.[15] Presumably this represents the effect of averaging the quadrupolar interaction over the orientational wave function. This means that the quadrupolar M_2 is about 30 times smaller than we compute classically. In order for the residual width of the NMR line due to quadrupolar interactions to be much less than the width we observe (about 2 kHz), we estimate that the correlation time t_c must be much shorter than 10^{-5} sec. This condition is certainly fulfilled at the temperature of the T_1 minimum reported in Ref. 15, where $t_c \simeq 10^{-7}$ sec. An analysis of the spin-lattice relaxation time in CH_4 II by Calvani and De Luca[22] supports the view that the correlation time remains short even at very low temperatures. In their theory, the low-temperature reorientation rate is assumed to be comparable to the tunneling matrix elements.

F. Spin-species conversion time

Nijman and Berlinsky[23] have computed the spin-species conversion time for CH_4 II at zero temperature. The processes they consider give extremely long conversion times for CD_4, because the tunneling splittings are much smaller than in CH_4. It is to be expected that the quadrupole interactions of the deuteron give rise to new conversion mechanisms which are much more efficient than the mechanisms operative in CH_4. If the dominant mechanism is a phonon emission process, the temperature dependence of the conversion rate τ^{-1} due to thermal phonons will be

$$\tau^{-1}(T) = \tau^{-1}(0)[1 + 2(e^{E/kT} - 1)^{-1}] , \quad (5)$$

where E is the energy of the emitted phonon. By fitting the observed spin-species conversion times to this formula, we may decide if first-order phonon emission is a plausible conversion mechanism. A similar phenomenological analysis was applied by the present authors to measurements of the spin-species conversion time in CH_4, resulting in the conclusion that there was excess thermally activated conversion over that expected for a phonon emission process.[24]

III. EXPERIMENTAL PROCEDURES AND RESULTS

A. The NMR spectrometer

The static magnetic field was supplied by a 7.5-T superconducting magnet. The frequency-swept rf spectrometer employed a commercial hybrid quadrature bridge. The sample was contained in a resonant circuit which was impedance matched to the 50-ohm rf bridge by a coupling loop. Small mismatches were introduced in the arm of the bridge opposite the resonant circuit, in order to cancel the dispersive component of the NMR line. Phase-sensitive detection synchronous with an applied magnetic modulation yielded derivative NMR lines. The output of the phase-sensitive amplifier was digitized by a microcomputer system, which provided a digital low-pass filter. The microcomputer was also used to control the frequency scan and to obtain the areas of the NMR lines by double integration. Figure 2 shows the sample chamber, which was cast of epoxy. A strong thermal link between the sample and dilution refrigerator mixing chamber is provided by 1500 copper wires 0.3 mm in diameter. There is 150 cm^2 of contact area per cm^3 of sample. The wires are insulated with Formvar to allow the rf field to penetrate the sample chamber.

B. Sample and condensation procedure

The sample was CD_4 from Merck, Sharp, and Dohme (Montreal) with an isotopic purity of 99.2%. It should be noted that the excess relaxation produced by paramagnetic impurities like O_2 is effectively frozen out at the high H/T values used in these experiments. The sample was condensed and frozen over the course of 2 h by gradually reducing the power supplied to the sample chamber heater, in the presence of a small amount of exchange gas coupling the chamber to the main liquid-helium reservoir of the cryostat. Once the temperature was well below the triple point, more exchange gas was introduced to cool the sample rapidly to 4.2 K.

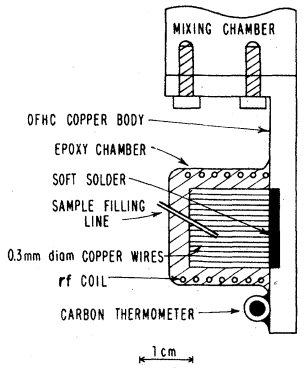

FIG. 2. Sample chamber and rf resonator.

C. Temperature calibration

The basic temperature reference was provided by a carbon resistance thermometer affixed to the copper arm connecting the sample-chamber wires to the refrigerator. The carbon thermometer had been previously calibrated against a germanium thermometer, in zero magnetic field. The known magnetoresistance of the carbon thermometer[25] allowed us to transfer the calibration to high field.

Because we were interested in measuring departures from the Curie law, it was particularly important to avoid the errors that may have accumulated during the multistep calibration process of the carbon thermometer. These errors become increasingly difficult to avoid at the lower dilution refrigerator temperatures, both because of the Kapitza boundary resistance between dissimilar materials and because of the extreme sensitivity of carbon thermometers to heating from extraneous rf fields and hum pickup. For these reasons, we calibrated the carbon thermometer using the Curie law for NMR on the copper wires in the sample chamber. In effect, the measured nuclear magnetic susceptibility of the deuterons in CD_4 was normalized to the susceptibility of the copper wires upon which the CD_4 was frozen.

D. NMR line area results

At the lower temperatures, the deuteron NMR line area showed a marked increase over that expected from the Curie law alone. This increase amounted to about 50% at 35 mK and was clearly distinguishable from temperature-dependent line area changes by the long time constant with which it was associated (about 2 h). In Fig. 3, the data points for each temperature show a sequence of NMR line areas obtained at regular time intervals after a sudden change in temperature. The sequences marked with an upward arrow were obtained after suddenly cooling the sample to the indicated temperature [the line area increases towards its new equilibrium value after such a change, because the equilibrium $\langle I(I+1)\rangle$ is greater for the lower temperature]. Similarly, the sequences marked with a downward arrow were obtained after suddenly warming the sample. The dashed line in Fig. 3 shows the Curie-law temperature dependence expected in the absence of spin-species conversion, while the solid line shows the smoothed equilibrium line area obtained by fitting the data to a model described below.

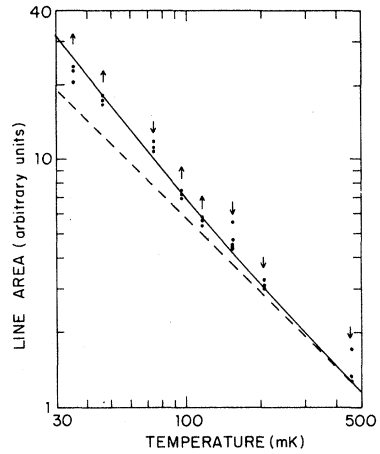

FIG. 3. NMR absorption line area as a function of temperature and time. The points for each temperature show a sequence of line areas measured after rapidly cooling (upwards arrows) or warming (downwards arrows) the sample to the indicated temperature. After such a change in temperature, the area showed a monotonic change with time in the direction indicated by the arrow. The points represent the area measured at 1-h intervals (for $T>150$ mK) or 2-h intervals (for $T<150$ mK). The solid line is the equilibrium line area derived by fitting the data to a model for the tunnel levels. The dashed line shows the temperature dependence predicted by the Curie law in the absence of spin conversion.

At each temperature T, the time-dependent sequence of line areas $A(t)$ was fit to an exponential relaxation:

$$A(t)=K_1(1-K_2e^{-t/\tau}) . \tag{6}$$

The conversion times τ obtained from this fitting procedure will be discussed in Sec. III G below. The value of K_2 in this expression depends upon the thermal history of the sample. The equilibrium line area K_1 obtained from this fit is proportional to $\langle I(I+1)\rangle/T$. The shaded bands in Fig. 4 show the temperature dependence of $\langle I(I+1)\rangle$ predicted by the five models of PPH [the width of each band indicates the range of the variation of $\langle I(I+1)\rangle$ among all five models]. One band shows $\langle I(I+1)\rangle$ averaged over all three spin species, as is appropriate if the F species NMR line is not highly broadened by quadrupole interactions. The other band shows the temperature dependence of $\langle I(I+1)\rangle$ which would be seen in an NMR experiment, if the F species were unobservable. The data points in Fig. 4 show $\langle I(I+1)\rangle$ computed from our NMR measurements. The data are shown twice: For the upper set of points, the unknown proportionality constant between line area and nu-

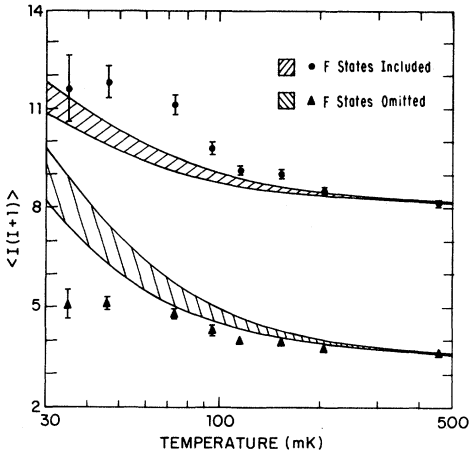

FIG. 4. Temperature dependence of $\langle I(I+1)\rangle$ predicted by the tunneling-level models of Ref. 10 (shaded bands) and $\langle I(I+1)\rangle$ derived from NMR line areas (data points). See text for detailed explanation.

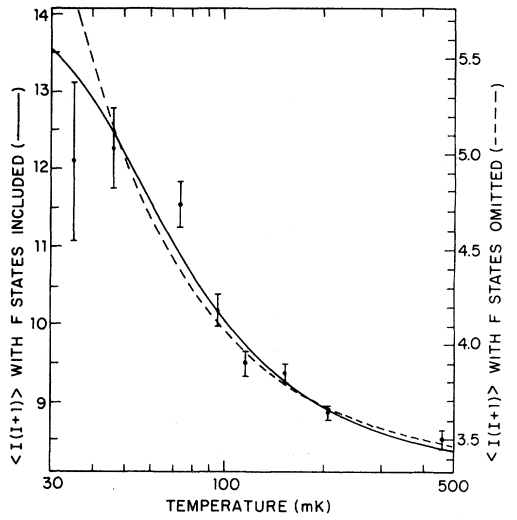

FIG. 5. Temperature dependence of $\langle I(I+1)\rangle$ predicted from model 0, with the tunneling splitting adjusted for best agreement with the data (solid and dashed curves), and $\langle I(I+1)\rangle$ derived from NMR line areas (data points).

clear susceptibility was adjusted to give agreement at 455 mK, the highest temperature observed, with the models with F states included. For the lower set of points the proportionality constant was adjusted to give agreement at 455 mK with the models with the F states assumed unobservable. The error bars include area measurement errors estimated from the fit to Eq. (6), as well as systematic errors in temperature measurement. The experimental points are not consistent with the models of PPH whether or not the F states are observable, although they are clearly closer to the curves which include the contribution from the F states.

It is clear from Fig. 4 that the present data do not have enough resolution to distinguish between the various multisite models of PPH. The data do provide a sensitive measure of the average tunneling splitting, however, and seem to indicate that this quantity is somewhat larger than for any of the five models (if the F states are observed). In view of this, we have fit the experimental line areas to the simple one-site model 0 described above. This model is described by the single adjustable parameter h, the sum of the four 120° overlap matrix elements. Figure 5 shows the best fit of the experimental data to model 0, under the two assumptions about the contribution of the F states. The data suggest that the F states do contribute to the NMR line. The fitting procedure resulted in a value of 59.9 ± 7.3 mK for $-h$ when the F states were included, and a value of 17.1 ± 2.1 mK when they were omitted. The latter value is difficult to reconcile with the energies of the neutron scattering transitions observed by PPH (up to 92 mK).

E. NMR linewidth results

Figure 6 shows the integrated and derivative NMR absorption lines observed at 35 and 455 mK.

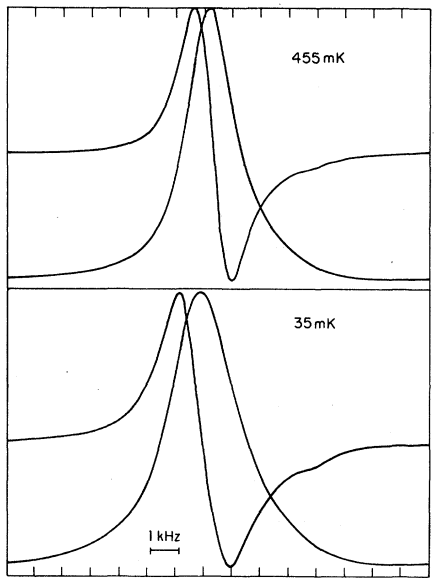

FIG. 6. Derivative and integrated NMR absorption lines at 455 and at 35 mK.

The NMR line shows a significant increase in width at the lower temperatures. Figure 7 shows the FWHM of the NMR line, measured after spin-species conversion was essentially complete at each temperature. The temperature dependence of the frequency separation between the peaks of the derivative line is also shown in Fig. 7. Figure 8 shows a graph of the experimental FWHM versus the square root of the second moment computed from Eqs. (2) and (4). The temperature-dependent probabilities for the three spin species were computed from our model 0, using the values of h obtained from the line area data. A straight line fit to the data in Fig. 8 gave the following relations between the FWHM ν and the computed second moments. For F states included [Eq. (2)],

$$\nu=(0.85\pm0.09)(M_2)^{1/2}+(0.31\pm0.20)\ , \qquad (7a)$$

and for F states omitted [Eq. (4)],

$$\nu=(2.4\pm0.2)(M_2')^{1/2}-(3.2\pm0.5)\ , \qquad (7b)$$

both in units of kHz. Note that any temperature-independent excess in the FWHM (caused, for example, by inhomogeneity in the magnetic field or by intramolecular interactions) would result in a positive constant term in these equations. The constant term in Eq. (7a) is consistent with zero. The unphysical negative constant term in Eq. (7b) is another indication that the F states probably contribute to the observed NMR line.

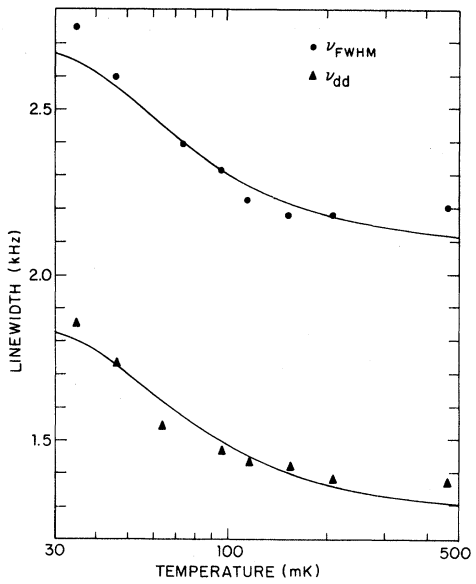

FIG. 7. Temperature dependence of the width of the NMR line at half maximum (ν_{FWHM}) and of the frequency separation of the peaks in the derivative line (ν_{dd}). The solid curves were derived by fitting the linewidths to a linear dependence on the square root of the computed second moment.

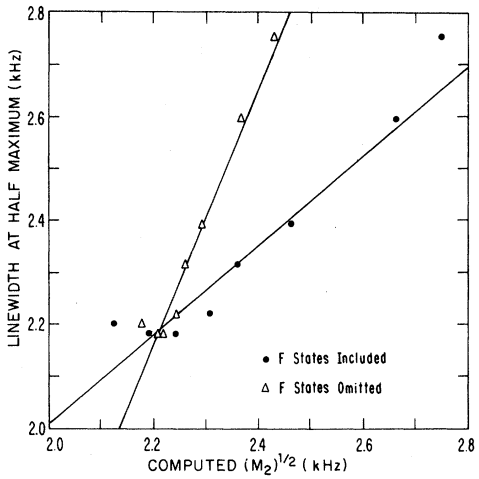

FIG. 8. Width of the NMR line at half maximum vs the square root of the intermolecular second moment computed from model 0 [Eqs. (2) and (4)]. The solid lines show the best fit to a straight line.

F. Spin-lattice relaxation time

Figure 9 shows the nuclear spin-lattice relaxation time T_1 obtained by observation of the recovery of the NMR signal after saturation (the relaxation times are for spin-species populations near their thermal equilibrium values). The relaxation rate is approximately proportional to the temperature in the range 42–455 mK, and appears to depend mainly upon the relative populations of the three spin species. If the main relaxation mechanism were the residual quadrupole interaction in the F species, then the A and E molecules would relax via

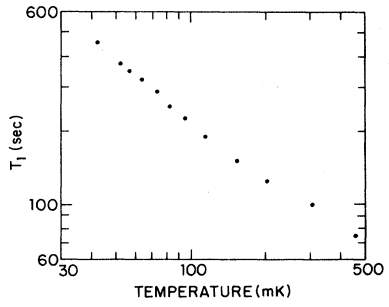

FIG. 9. Spin-lattice relaxation time T_1 as a function of temperature.

spin exchange with the F molecules, thus explaining the dependence of T_1 on spin-species populations. However, the temperature dependence of the equilibrium T_1 would then be much stronger than we observe. A comparison of our measurements with those of de Wit and Bloom[15] is roughly consistent with a single-correlation-time model for molecular reorientations, which predicts a low-temperature relaxation time proportional to the square of the Larmor frequency.

G. Spin-species conversion time results

Figure 10 shows the spin-species conversion time τ obtained by fitting the measured NMR line area to Eq. (6). While we do not have a theory of nuclear-quadrupole-induced conversion, we have fit the data to the form expected for a phonon emission process, Eq. (5). The data are insufficient to yield an unambiguous value for the phonon energy E that appears in Eq. (5). The two curves in Fig. 10 were computed using the values of the A-F splitting obtained from fitting the observed $\langle I(I+1)\rangle$, under the two assumptions about the observability of the F states (120 and 34 mK). Both curves are consistent with the data. This may be contrasted with the case of CH_4 II, where it was found that the spin-species conversion time of the free-rotor molecules had a more rapid temperature dependence than was consistent with a phonon emission process.[24]

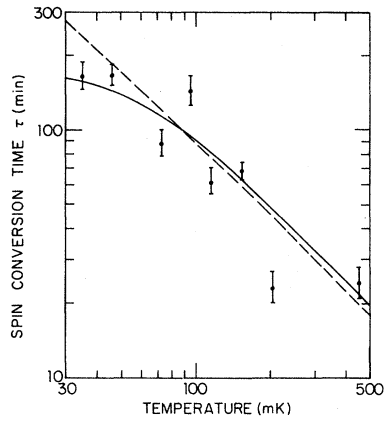

FIG. 10. Spin-species conversion time as a function of temperature. The solid line shows the temperature dependence expected for a phonon emission process, using a tunnel splitting derived under the assumption that the F species molecules contributed to the observed NMR line. The dashed line shows the dependence computed under assumption that the F molecules were unobserved.

IV. CONCLUSIONS

The present NMR line area measurements provide clear evidence for the existence of tunneling states in CD_4 III with splittings on the order of 100 mK. The average tunneling splitting we obtain is about 50% larger than that obtained by PPH on the basis of neutron scattering. Both line area and linewidth data suggest that the F spin species contributes a narrow NMR line, presumably due to rapid collective transitions among the F substates. Our high-field measurements of the spin-lattice relaxation time are roughly consistent with the low-field measurements of de Wit and Bloom[15] if the correlation time for transitions between the F substates is assumed to be longer than the Larmor periods but shorter than the inverse NMR linewidth. Spin-species conversion times on the order of two hours are observed. The temperature dependence of the conversion time is consistent with that expected for a phonon emission process.

The quadrupole moment of the deuteron gives rise to mechanisms for spin-species conversion and for spin-lattice relaxation which are not present in CH_4. It would be desirable for the existing theories of these processes[20–23] to be extended to take these new mechanisms into account.

ACKNOWLEDGMENT

This work was supported by the National Science Foundation under Grant No. DMR 79-07023.

[1]T. Nagamiya, Prog. Theor. Phys. 6, 702 (1951).
[2]A. Huller and D. M. Kroll, J. Chem. Phys. 63, 4495 (1975).
[3]J. H. Colwell, E. K. Gill, and J. A. Morrison, J. Chem. Phys. 39, 3 (1963).
[4]H. M. James and T. A. Keenan, J. Chem. Phys. 31, 12 (1959).
[5]T. Yamamoto, Y. Kataoka, and K. Okada, J. Chem. Phys. 66, 2701 (1977).
[6]H. Glattli, A. Sentz, and M. Eisenkremer, Phys. Rev.

Lett. 28, 871 (1972); B. Bouchet and H. Glattli, J. Phys. (Paris) Lett. 42, L159 (1981).
[7]W. Press and A. Kollmar, Solid State Commun. 17, 405 (1975).
[8]A. Huller and J. Raich, J. Chem. Phys. 71, 3851 (1979).
[9]K. Maki, Y. Kataoka, and T. Yamamoto, J. Chem. Phys. 70, 655 (1979).
[10]M. Prager, W. Press, and A. Heidemann, J. Chem. Phys. 75, 1442 (1981).
[11]E. A. Ballik, D. J. Gammon, and J. A. Morrison, J. Chem. Phys. 58, 5639 (1973).
[12]M. A. White and J. A. Morrison, J. Chem. Phys. 72, 5927 (1980).
[13]W. Press, M. Prager, and A. Heidemann, J. Chem. Phys. 72, 5924 (1980).
[14]A. Huller, Phys. Rev. B 16, 1844 (1977).
[15]G. A. de Wit and M. Bloom, Can. J. Phys. 47, 1195 (1969).
[16]C. H. Anderson and N. F. Ramsey, Phys. Rev. 149, 14 (1966).
[17]J. E. Piott and W. D. McCormick, Can. J. Phys. 54, 1799 (1976).
[18]A. J. Nijman and N. J. Trappeniers, Physica 95B, 147 (1978).
[19]A. Abragam, *The Principles of Nuclear Magnetism* (Oxford University Press, London, 1961).
[20]A. J. Nijman, M. Sprik, and N. J. Trappeniers, Physica 98B, 247 (1980).
[21]M. Sprik and N. J. Trappeniers, Physica 103A, 411 (1980).
[22]P. Calvani and F. De Luca, J. Chem. Phys. 73, 167 (1980).
[23]A. J. Nijman and A. J. Berlinsky, Phys. Rev. Lett. 38, 408 (1977).
[24]S. Buchman, D. Candela, W. T. Vetterling, and R. V. Pound, Phys. Rev. B 26, 1459 (1982).
[25]H. H. Sample, L. J. Neuringer, and L. G. Rubin, Rev. Sci. Instrum. 45, 58 (1974).